Received: June 24, 2015 Revised: August 3, 2015 Accepted: August 5, 2015

(onlinelibrary.wiley.com) DOI: 10.1111/ner.12346

Spinal Cord Stimulation (SCS) and Functional Magnetic Resonance Imaging (fMRI): Modulation of Cortical Connectivity With Therapeutic SCS

Milind Deogaonkar, MD[1]*; Mayur Sharma, MD[1]*; Chima Oluigbo, MD[†]; Dylan M. Nielson, PhD[‡]; Xiangyu Yang, PhD[§]; Louis Vera-Portocarrero, PhD[¶]; Gregory F. Molnar, PhD[¶]; Amir Abduljalil, PhD[§]; Per B. Sederberg, PhD[‡]; Michael Knopp, MD[§]; Ali R. Rezai, MD*

Introduction: The neurophysiological basis of pain relief due to spinal cord stimulation (SCS) and the related cortical processing of sensory information are not completely understood. The aim of this study was to use resting state functional magnetic resonance imaging (rs-fMRI) to detect changes in cortical networks and cortical processing related to the stimulator-induced pain relief.

Methods: Ten patients with complex regional pain syndrome (CRPS) or neuropathic leg pain underwent thoracic epidural spinal cord stimulator implantation. Stimulation parameters associated with "optimal" pain reduction were evaluated prior to imaging studies. Rs-fMRI was obtained on a 3 Tesla, Philips Achieva MRI. Rs-fMRI was performed with stimulator off (300TRs) and stimulator at optimum (Opt, 300 TRs) pain relief settings. Seed-based analysis of the resting state functional connectivity was conducted using seeds in regions established as participating in pain networks or in the default mode network (DMN) in addition to the network analysis. NCUT (normalized cut) parcellation was used to generate 98 cortical and subcortical regions of interest in order to expand our analysis of changes in functional connections to the entire brain. We corrected for multiple comparisons by limiting the false discovery rate to 5%.

Results: Significant differences in resting state connectivity between SCS off and optimal state were seen between several regions related to pain perception, including the left frontal insula, right primary and secondary somatosensory cortices, as well as in regions involved in the DMN, such as the precuneus. In examining changes in connectivity across the entire brain, we found decreased connection strength between somatosensory and limbic areas and increased connection strength between somatosensory and DMN with optimal SCS resulting in pain relief. This suggests that pain relief from SCS may be reducing negative emotional processing associated with pain, allowing somatosensory areas to become more integrated into default mode activity.

Conclusion: SCS reduces the affective component of pain resulting in optimal pain relief. Study shows a decreased connectivity between somatosensory and limbic areas associated with optimal pain relief due to SCS.

Keywords: Connectivity, functional MRI, neural networks, neuromodulation, neuropathic pain

Conflict of Interest: Louis Vera-Portocarrero and Gregory F. Molnar are employees of Medtronic and have financial interest in Medtronic plc.

INTRODUCTION

Neuropathic pain is defined as "pain initiated or caused by a primary lesion or dysfunction in the nervous system" (1,2). Chronic neuropathic leg pain is the most common form of neuropathic pain with an estimated annual prevalence between 9.9% and 25% in the general population (3,4). According to the International Association for Study of Pain (IASP), the diagnostic criterion for complex regional pain syndrome (CRPS) type 1 includes the presence of disproportionate persistent pain with allodynia or hyperalgesia; presence of inciting noxious event or immobilization; presence of edema, changes in blood flow, or abnormal sudomotor activity in the region of the pain; absence of obvious cause of the degree of pain and dysfunction (5). Spinal cord stimulation (SCS) is a well-established therapeutic option for patients with refractory chronic back and

Address correspondence to: Milind Deogaonkar, MD, Department of Neurosurgery, Center of Neuromodulation, Wexner Medical Center, The Ohio State University, 480 Medical Center Drive, Columbus, OH 43210, USA. Email: Milind.Deogaonkar@osumc.edu

* Department of Neurosurgery, Center of Neuromodulation, Wexner Medical Center, The Ohio State University, Columbus, OH, USA;
† Department of Neurosurgery, Children's National Medical Center, Washington, DC, USA;
‡ Department of Psychology, The Ohio State University, Columbus, OH, USA;
§ Department of Radiology, Wexner Medical Center, The Ohio State University, Columbus, OH, USA; and
¶ Neuromodulation Research, Medtronic Inc., Minneapolis, MN, USA

For more information on author guidelines, an explanation of our peer review process, and conflict of interest informed consent policies, please go to http://www.wiley.com/WileyCDA/Section/id-301854.html

[1] These authors contributed equally to this work.

neuropathic leg pain (6–10). The neurophysiological basis, neural correlates, and mechanism of pain relief due to SCS are important areas of investigation. Multiple spinal segmental and supraspinal mechanisms have been implicated in the neurophysiological basis of SCS in alleviating chronic pain (11–16). Nonuniformity of pain relief with SCS in spite of good paresthesia coverage points to central neuromodulation of pain networks. The neuromatrix theory of pain also proposed that pain perception varies according to cognitive, emotional, and sensory influences (17,18). Melzack proposed the neuromatrix theory of pain, which comprised of neural networks with somatosensory, limbic, and thalamocortical components subserving the sensory, affective, and cognitive components of pain (17). The output of this neuromatrix in terms of pain perception and behavior is unique to an individual and determined by the genetic makeup and sensory experiences. Sensory inputs that modulate the neuromatrix and the output include somatosensory inputs from different peripheral sensory receptors, visual, cognitive, emotional inputs, brain inhibitory pathways, and stress regulating pathways (autoimmune, endocrine, and autonomic) (17).

Functional magnetic resonance imaging (fMRI) is a powerful tool for understanding and mapping the areas of brain involved in pain perception and modulation such as somatosensory cortex, limbic areas, and resting mode networks (19,20). Understanding neural networks implicated in the pathophysiology of pain in turn lead to development of newer modalities to manage chronic persistent pain (21). Functional neuroimaging has shown that central processes such as memory and learning-related changes in the pain pathways/networks with altered perception of body image have been implicated in the pathophysiology of chronic pain perception (21). The use of fMRI in delineating cortical or subcortical activation during SCS has been reported by very few investigators (22–24). Kiriapopoulus et al. (22) reported fMRI activation of the primary and secondary somatosensory cortices during SCS in three patients with failed back surgery syndrome (FBSS). Increased fMRI activation of the medial primary and sensorimotor cortex somatotopically corresponding to the foot and perineal region, contralateral posterior insula, and the ipsilateral secondary somatosensory cortex was reported in eight patients treated with SCS for neuropathic back and leg pain in FBSS (23). Another study reported activation in the primary and secondary somatosensory area, cingulate gyrus, thalamus, prefrontal cortex in three patients with SCS for FBSS (24).

The main objective of this study was to assess patterns of fMRI cortical and subcortical blood oxygen level dependent (BOLD) activation with SCS in patients with neuropathic leg pain and define changes in cortical networks and cortical correlates of pain relief in the setting of neuropathic leg pain.

MATERIALS AND METHODS

This prospective study was approved by the Institutional Review Board and was carried out in accordance with the Health Insurance Portability and Accountability Act (HIPAA). A total of ten patients were enrolled in this study over a period of one year. Participants for the study were recruited from a pool of patients who already had thoracic epidural spinal cord stimulator either for the treatment of neuropathic leg pain involving one or both lower extremities following FBSS or CRPS (diagnosed by the pain management team using standard scales) (5,25). Patients had their SCS implanted either at Ohio State University and Wexner Medical Center or at an outside facility. Prospective participants had to satisfy the following inclusion and exclusion criteria in order to join this study.

Inclusion Criteria

The following are the inclusion criteria for this study:

1. Age between 18–65 years at the time of enrollment in the study.
2. Had previous implantation of thoracic epidural Medtronic (Medtronic, Inc., Minneapolis, MN, USA) Restore Ultra, Prime Advanced and Restore Advanced SCS for the treatment of CPRS-type 1 or chronic refractory neuropathic leg pain following FBSS. The implantation must be three or more months prior to enrollment.
3. Unilateral or bilateral lower extremity pain.
4. Patients must have reported significant pain improvement (>50%) following SCS implantation.
5. Patients must have reported consistently reproducible pain relief (>50%) within 10 min of switching SCS from an OFF state to an ON state (with "optimal" parameters).
6. The SCS pulse generator is implanted in the buttocks region.
7. Patients must be able to provide informed and valid consent.

Exclusion Criteria

The following are the exclusion criteria for this study:

1. Contraindication to MRI such as presence of cardiac pacemaker, metallic implants, intracranial aneurysm clips, external clips within 10 mm of the head, metallic foreign metals within the orbits, spinal cord stimulator within the cervical epidural region.
2. Positive pregnancy test on urine analysis.
3. Claustrophobic patient.
4. Inconsistent response of pain to SCS or long interval (>10 min) before pain relief following switching SCS from an OFF state to an ON state (with "optimal" parameters)—long "washout" period or lack of significant pain improvement (<50%) following implantation of SCS.
5. History of prior ablative neurosurgery or large vessel stroke or brain tumors.
6. Evidence of personality or other psychiatric disorders, dysfunctional behavior, consumption of recreational drugs/alcohol abuse.

Preimaging Clinical Evaluation

Following written informed and valid consent, each of the participants was clinically evaluated one week prior to the acquisition of functional imaging. The clinical evaluation was performed to determine the stimulation parameters associated with "optimal" pain reduction and spinal cord stimulator perception threshold.

Stimulation parameter refers to the combination of electrode contacts, pulse frequency, width and voltage level that was taken from the handheld SCS programmer. The method for determining "optimal" pain reduction with SCS is described below. Once the "optimal" parameters were identified, the voltage level was titrated to achieve optimal pain reduction prior to fMRI. All determinations were made with the patient in supine position. It was also at this preimaging clinical evaluation that patients were assessed for consistently reproducible response of their pain to SCS and the time interval between switching the SCS from an OFF state to an ON state at optimal parameter settings and reduction in pain in less than 10 min. To avoid the potential confounding element of lingering effects of chronic stimulation (24), the subjects were asked to turn off their stimulators two hours before the preimaging clinical evaluation. Patients were also asked to refrain from taking analgesics at least 24 hours prior to testing.

Pain Quantification and Determination of Optimal Parameters

Pain quantification was done using the visual analog scale (VAS). The VAS is a reliable and validated nonverbal rating scale used for assessing the pain and disability (26–28). This scale ranges from "0" being "no pain at all" to "10" being "the worst pain imaginable." Subjects were instructed to draw a vertical line on a 10 cm horizontal scale to determine their pain level. The measure of percentage change in pain (ΔP%) was determined as follows:

$$\Delta P\% = 100 \times (P_{OFF} - P_{ON})/P_{OFF}$$

where P_{ON} was the VAS pain rating as reported by the subject during stimulation ON and P_{OFF} was the pain rating reported with the stimulator turned OFF.

Optimal pain reduction parameter (in the supine position) represents the parameter that resulted in the best pain relief as evidenced by the greatest ΔP%. In many of these patients who had the SCS in place, optimal settings were already established and those parameters were used in such situations.

Imaging Acquisition and Analysis

The clinical evaluation in the form of baseline pain quantification was performed using the VAS prior to fMRI.

General fMRI Protocol

The subjects were placed inside the MRI scanner in the transmit/receive head coil. A scout image and an anatomic 3D image dataset were acquired using the parameters outlined below. Functional imaging exams were performed using a simple block style paradigm that alternates between the stimulator "OFF" condition and the stimulator "optimal" condition with settings delivered at the predetermined "optimum" stimulation parameters.

There was a single 10-min epoch in each of the above stimulator conditions. Stimulation settings were changed between collections of scans. Patients were closely monitored throughout the experiment, and instructed to immediately report any discomfort or sensation of heat in their back, either during preparation for the MR examination or during actual scanning.

fMRI Recordings and Data Analysis

Images were acquired using a 3 Tesla MRI system (Philips Achieva, Amsterdam, The Netherlands) equipped with a transmit and receive head coil. Functional images were acquired using a blipped single-shot gradient-echo EPI imaging sequence with a spatial resolution of 2.75 × 2.75 × 3.5 mm. The acquisition parameters were: TR/TE 2000/24 ms, 80° flip angle, 64 × 64 matrix size, 220 × 220 mm field of view, 30 slices, and echo train of 35 ms. The number of dynamic acquisitions was 300 and the total scan time was 6 min for each rs-fMRI session. A high resolution T1 weighted image was also acquired with the following parameters: TR/TE 8.1/3.7 ms, 1 × 1 × 1 mm^3 voxel resolution, 3D acquisition with 118 slices, 7.5 min total scan time. In addition, an image set with similar resolution to the functional scan and with two gradients recalled echoes were used to measure the B0 inhomogeneity map. The time between the two echoes was 1.4 ms.

Image Processing for Seed-Based Analysis

All data were spatially filtered with a Hamming filter that has been demonstrated to provide a threefold increase in signal-to-noise. The MRI time series at each pixel was fit using least squares to a boxcar reference function plus a slope and intercept to generate Student's *t* maps. A Talairach transformation was then performed on the anatomical data and Student's *t* maps. Student's *t* maps were superimposed on the anatomical datasets and analyzed for areas of activation. A threshold value of $t = 3.5$ ($p < 10^{-3}$) was used to determine voxels of significant activation. The Talairach coordinates of the centroid for regions of significant activation were used to determine anatomic location. Additionally, activation was also determined using region of interests (ROIs) determined from the anatomic imaging scan.

Images from all ten recruited patients were analyzed individually, with each patient serving as his/her own control because of variability of symptoms and emotional manifestations of pain across different patients. An analysis of ROIs across subjects was performed to assess for consistency of regions of activation in particular pain syndromes such as CRPS vs. FBSS with neuropathic leg pain. Seed-based analysis of the resting state functional connectivity was conducted using seeds in regions linked to the pain networks or in the default mode network (DMN).

Image Processing for Network Analysis

Anatomical and resting state functional images were processed using modified versions of the 1000 Functional Connectomes processing scripts (29). These scripts utilize FSL (30) and AFNI (31) to prepare functional images for resting state analysis. The functional images were motion corrected, smoothed with a 5 mm Gaussian kernel, and band pass filtered to remove frequencies below 0.0005 Hz and above 0.1 Hz. Linear trends were removed to correct for scanner drift; nuisance signals, including white matter, cerebrospinal fluid (CSF), and primary visual cortex signals, were regressed out and the images were scaled to a mean of 100. Functional images were linearly registered to anatomical space using a rigid affine transformation. Anatomical images were nonlinearly registered to 2 mm MNI-152 space. This nonlinear transformation was applied to the functional images to move them into standard space.

Seed-Based Functional Connectivity Analysis

Seeds with a radius of 6 mm were placed at each of the coordinates listed in Table 1, corresponding to structures implicated in pain networks or the DMN (32). The time course from each of these regions was extracted and the correlation coefficient was calculated with the functional time course at each voxel within subject. These correlation coefficients were *z* transformed and a *t*-test was ran across subjects to identify voxels with a correlation coefficient significantly different between the off and optimal state. We used fdrtool (33) to control the total false discovery rate at less than or equal to 5% across statistical maps for all of the seeds examined, and only clusters of 50 mL or larger were kept. The *t*-values for voxels surpassing this false discovery rate and cluster size threshold were displayed on the MNI-152 template using MRIcroGL. In order to preserve statistical power, only the contrast between the off and optimal settings was analyzed.

Whole Brain Connectivity Analysis

In order to identify changes in functional connectivity related to SCS in regions beyond those identified in previous studies, we utilized the normalized cut (NCUT) method to identify 100 contiguous, functionally distinct gray matter regions based on the functional

Table 1. Seeds Used for Seed Based Analysis of Functional Connectivity Changes With Spinal Cord Stimulation.

Network	Region of interest	x (mm)	y (mm)	z (mm)
Pain related	Left dorsolateral prefrontal cortex	−34	31	34
Pain related	Right dorsolateral prefrontal cortex	44	36	20
Pain related	Frontal medial cortex	0	42	−18
Pain related	Left orbital frontoinsula	−32	24	−10
Pain related	Right orbital frontoinsula	38	26	−10
Pain related	Left nucleus accumbens	−10	12	−8
Pain related	Right nucleus accumbens	10	10	−8
Pain related	Left amygdala	−20	−6	−20
Pain related	Right amygdala	28	−6	−20
Pain related	Left posterior insula	−39	−24	16
Pain related	Right posterior insula	38	14	6
Pain related	Left anterior cingulate cortex	−2	36	6
Pain related	Right anterior cingulate cortex	6	38	14
Pain related	Left thalamus	−14	−16	8
Pain related	Right thalamus	10	−19	6
Pain related	Left primary somatosensory cortex	−32	−40	63
Pain related	Right primary somatosensory cortex	20	−49	67
Pain related	Left secondary somatosensory cortex	−52	−24	20
Pain related	Right secondary somatosensory cortex	52	−26	22
Task positive network	Intraparietal sulcus	−38	−46	54
Task positive network	Frontal eye field	26	−12	50
Task positive network	Middle temporal gyrus	−48	−68	−2
Default mode network	Medial prefrontal cortex	−2	46	16
Default mode network	Posterior cingulate/precuneus	6	38	14
Default mode network	Lateral parietal cortex	−46	−68	36

Coordinates are given in MNI space.

connectivity. Twenty-seven of these regions were in the occipital lobe and were removed from subsequent analyses to preserve statistical power. For each subject, the time course was extracted for each of the remaining 73 ROIs and the correlation between that time course and the time course from every other ROI was calculated, yielding a 73 by 73 matrix of correlation coefficients for each subject. These were *z* transformed and *t*-tests were conducted across subjects comparing the off and optimal settings. We again used fdrtool (33) to control the false discovery rate at less than or equal to 5%. We then used Circos to visualize the significant changes in functional connectivity. Again, in order to preserve statistical power, only the contrast between the OFF and optimal settings was analyzed.

Statistical Analysis of Multisubject fMRI Data

Statistical analysis was performed to assess for consistency of regions of activation, in particular pain syndromes such as CRPS vs. FBSS with neuropathic leg pain. In the first step, a voxel-wise *t*-test across standardized *z*-maps was performed to identify areas that were consistently activated across subjects. In the second step, for each area, individual mean *z*-scores were calculated and subsequently subjected to an analysis of variance. NCUT parcellation (34) was used to generate 98 cortical and subcortical ROIs in order to expand our analysis of changes in functional connections to the entire brain (34) (Fig. 1). We corrected for multiple comparisons by limiting the false discovery rate to 5%.

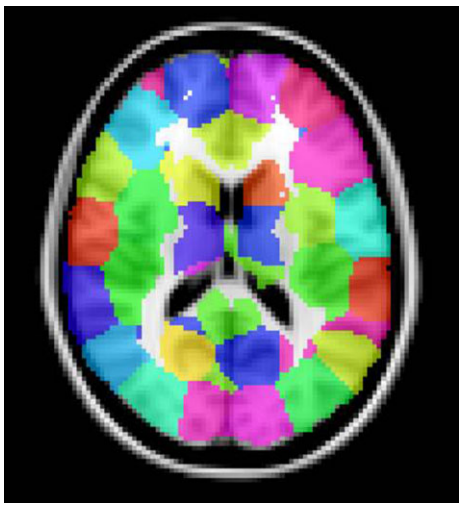

Figure 1. Functional parcellation map using time series data concatenation with gray matter parcellation into 98 regions of interest (ROIs) using normalized cut (NCUT).

RESULTS

Ten patients (6 men/4 women, aged 35–64 years) with neuropathic pain who had SCS placed more than three months ago were enrolled in this study. The average percentage change in pain (ΔP%) with optimum stimulator settings was 45% (minimum change = 0%, maximum change 75%) (Table 2). The second patient with 0% pain relief had 50 to 60% benefit after stimulator placement, but on the day of study with his optimal settings we could not replicate it because he took his pain medications just before the study.

There were no adverse effects with SCS and fMRI in all patients during the study.

Table 2. Table Showing the Diagnosis, Pain Location, Pain Duration, Pre-SCS Treatment, Location of Stimulator Leads Percentage Pain Relief With Spinal Cord Simulator Using Optimum Stimulator Settings at the Time of Study.

Subject	ΔP%	Diagnosis	Duration of pain in years	Pre-SCS treatment	Pain location	Top of stimulator lead
1	40	FBSS	10	Surgery, blocks, meds	Both legs	T8
2	0	CRPS	5	Blocks, meds	Right leg	T9
3	29	CRPS	14	Blocks, meds	Left leg	T8
4	71	FBSS	6	Surgery, blocks, meds	Both legs	T7
5	50	FBSS	8	Surgery, blocks, meds	Left leg and back	T8
6	27	CRPS	18	Blocks, meds	Right leg	T8
7	75	FBSS	15	Surgery, blocks, meds	Both legs	T8
8	30	FBSS	16	Surgery, blocks, meds	Both legs	T8
9	70	Neuropathic pain	4	Blocks, meds	Thoracic wall	T6
10	60	FBSS	9	Surgery, blocks, meds	Right leg	T9

CRPS, complex regional pain syndrome; FBSS, failed back surgery syndrome; SCS, spinal cord stimulation.

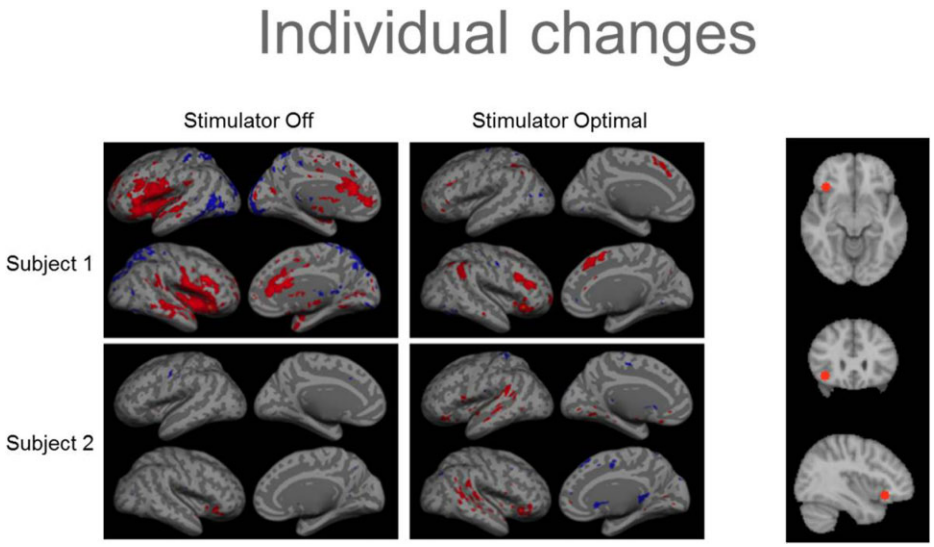

Figure 2. On an individual level, between the states of stimulator OFF and optimal stimulation, the greatest change in connectivity occurred when the right and left insula were selected as seeds. As can be seen, in the optimum stimulation state, there was reduction in connectivity on average across the board. The reduction in connectivity on the right as can be seen was in the medial prefrontal cortex and lateral parietal cortex which are part of the default mode network.

We have analyzed our data at both individual level and group level as described in a previous study (35). At individual level, the activity in each ROI was correlated with activities in other ROIs. Correlation was calculated using Pearson's correlation coefficient and statistical maps were created. We noted that between the states of stimulator OFF and optimal stimulation, the greatest change in connectivity occurred when the right and left insula were selected as seeds. In the optimum stimulation state, there was reduction in connectivity on average across the board (Fig. 2). The reduction in connectivity on the right as can be seen was in the medial prefrontal cortex and lateral parietal cortex, which are part of the DMN. Significant differences in resting state brain connectivity were seen between several regions related to pain perception, including the left frontal insula, right primary and secondary somatosensory cortices, as well as in regions involved in the DMN, such as the precuneus. At group level, the changes in resting state connectivity from stimulator optimal to OFF stimulation were seen in left frontal insula and precuneate area (Fig. 3).

Seed-Based Functional Connectivity

We observed differences in functional connectivity between the off and optimal states across the majority of the seeds we examined, representing nodes of both the default mode and pain networks (Table 3). The precuneus had the increased connectivity across the largest swath of cortex of any of the seeds examined, including increased connectivity with the cingulate cortex bilaterally and the DorsoLateral Prefrontal Cortex bilaterally, as well as decreased connectivity with regions in the right temporal lobe. The strongest decrease in connectivity between the off and optimal settings was observed between the right secondary somatosensory cortex and the left inferior parietal lobule (*t*-value = −14.2).

Whole Brain Connectivity Analysis

After using an NCUT method to divide the brain into 98 regions, we observed changes in functional connectivity between the off and optimal conditions in many regions (Fig. 4, Table 4). The

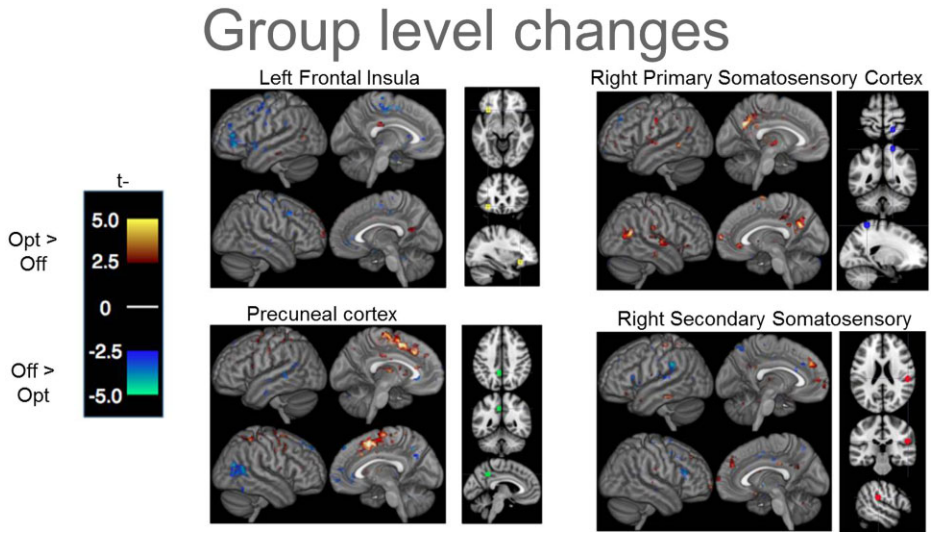

Figure 3. At group level, the changes in resting state connectivity from stimulator OFF to optimal stimulation were seen in left frontal insula and precuneate area. Red is optimal greater than off; blue off is greater than on.

strongest decrease in functional connectivity was between the left secondary somatosensory cortex and the right middle cingulate (*t*-value = –4.89). The greatest increase in functional connectivity was between the left superior precentral cortex and the left supramarginal cortex. The general trend of the results is decreased connectivity between somatosensory areas and limbic/emotional networks with increased integration of somatosensory regions into the DMN.

In group-level analysis, we also noted that connectivity during the resting state changes with the left frontal insula as a connectivity seed when the stimulation was turned from OFF to optimal state (Fig. 3). These seed regions were chosen based on regions typically involved in pain matrix/ pain networks.

We also did average pairwise correlation between 98 ROIs during the stimulator OFF and optimal state (Fig. 5). Regions that showed increases or decreases in correlation by 0.2 were averaged across the subjects. Average change in correlation across all subjects during the stimulator OFF and optimal state is seen in Figure 6.

DISCUSSION

Perception of pain and pain relief is closely connected to limbic networks and DMN in addition to somatosensory areas. The emotional processing of pain is routed through the limbic networks. This study shows that optimal pain relief is associated with modulation of network connectivity between the somatosensory and limbic network as well as DMN. Using Circos plots, the changes in functional connectivity between the ROIs during the stimulator OFF and optimal state have been demonstrated in Figure 4. The functional connectivity between the somatosensory and the limbic area showed a decreased strength with an increase in connectivity between somatosensory and the DMN when the patients had optimal stimulator settings. This decrease in somatosensory and limbic links and increase in somatosensory to DMN links mean that the patients were less tied to emotional processing and there was a sensation of pain relief during optimal stimulation. In other words, during inappropriate pain control or stimulator OFF settings, the limbic areas showed strong functional connectivity with the somatosensory cortex.

Functional neuroimaging such as fMRI and Positron Emmision Tomography scans are useful in elucidating the effects of SCS on supraspinal (cortical) processing of sensory information and unveiling the antinociceptive mechanisms. Previous studies have demonstrated the utility of fMRI in delineating the cortical or subcortical activation during SCS in patients with chronic neuropathic pain (22–24). In our study, increased connectivity was noted between left superior marginal and left superior precentral cortices, right middle frontal and left middle precentral cortices, left posterior cingulate and left superior frontal cortices, anterior cingulate and right medial prefrontal cortices, in decreasing order of strength at optimal stimulator settings. Increased connectivity was noted between right middle cingulate cortex and left somatosensory (S2) cortex, left anterior insula and left caudate in decreasing order of strength when the stimulator was turned OFF. Another fMRI study investigated the pattern of cerebral activation during SCS therapy in eight patients with FBSS. In this study, they noted increased activation of the medial primary sensorimotor cortex (foot and/or perineal region), contralateral posterior insula, and the ipsilateral secondary somatosensory cortex (S2) during SCS therapy (23). Decreased activation of the primary motor cortices on both sides and ipsilateral somatosensory cortex (shoulder, elbow, and hand) was also noted following SCS in this study (23). They also applied heat pain (HP) to the leg affected by neuropathic pain and noted that simultaneous HP and SCS showed statistically significant fMRI activation of bilateral paralimbic association cortex and ipsilateral cerebellum when compared with the sum of individual activations during SCS or HP stimulation (23). They hypothesized that SCS affects cortical and limbic processing of neuropathic pain and continuous comparison of simultaneous pain and SCS in the same dermatome results in greater activation of pain processing areas (23). Kiriakopoulos et al. (22) reported activation of S1 and S2 cortices in the right hemisphere following SCS (T11–T12 level) in a 43-year-old woman with neuropathic leg pain following FBSS. Bilateral activation of S1, S2, and cingulate regions in a patient with CRPS and sensory cortex activation in a patient with chronic

Table 3. Results of Seed-Based Analysis of Functional Connectivity Changes With Spinal Cord Stimulation Between Off and Optimal Settings.

Network	Seed	Region	Size	Peak				Center of mass		
				t	x	y	z	x	y	z
Task positive network	Frontal eye field	Right postcentral gyrus	76	−7.815	64	−26	16	61.5	−27.6	15.2
Task positive network	Frontal eye field	Left superior temporal gyrus	45	−6.467	−52	−40	16	−54.9	−39.7	14.2
Pain	Frontal medial cortex	Left cingulate gyrus	110	−7.179	−6	20	46	−3.9	21.1	46.3
Pain	Frontal medial cortex	Left thalamus, left ventral posterior lateral nucleus	49	−6.148	−18	−18	6	−17.5	−21.1	8.1
Pain	Frontal medial cortex	Left anterior cingulate, left caudate head	31	−5.694	−12	22	−2	−9.8	20.1	0.9
Task positive network	Intraparietal sulcus	Left superior temporal gyrus	45	−7.228	−48	−22	4	−46.4	−20.1	4.9
Task positive network	Intraparietal sulcus	Right inferior parietal lobule	28	−7.551	66	−30	34	65.8	−30.5	33.3
Task positive network	Intraparietal sulcus	Left superior frontal gyrus	28	9.837	−65	18	54	−37.3	18.7	54.3
Pain	Left nucleus accumbens	Left anterior cingulate	55	6.154	−6	24	18	−6.3	33	19.4
Pain	Left nucleus accumbens	Right superior frontal gyrus	26	6.553	20	50	30	21.2	48.8	31.3
Pain	Left anterior cingulate cortex	None								
Pain	Left amygdala	Left middle frontal gyrus, left Brodmann area 6 (leg area)	95	−7.226	−2	−30	66	−3	−33.5	60
Pain	Left dorsolateral prefrontal cortex	Left thalamus, near pulvinar and parahippocampal gyrus	61	7.164	−8	−34	2	−9.9	33.1	0.4
Pain	Left orbital frontoinsula	Left inferior frontal gyrus, left Brodmann area 46	49	−6.308	−44	44	12	−46.3	41.4	4.1
Pain	Left orbital frontoinsula	Left parahippocampal gyrus	34	−5.823	−36	−8	−28	−40	6.4	−22
DMN	Lateral parietal cortex	Right inferior parietal lobule, right Brodmann area 40	92	7.469	56	−34	42	55.6	−34.2	40.4
DMN	Lateral parietal cortex	Left cingulate gyrus, left Brodmann area 31	63	7.044	−4	−34	42	−4.2	−31.4	38.7
DMN	Lateral parietal cortex	Right superior temporal gyrus, right Brodmann 42	28	8.169	56	−32	14	55.1	−33.3	9.7
Pain	Left posterior insula	Left precentral gyrus, left Brodmann area 6	47	−7.495	−44	−6	38	−42.5	−4.9	38.1
Pain	Left posterior insula	Right subcallosal gyrus (near right nucleus accumbens)	25	6.124	12	10	−12	11.5	11.7	−12.8
Somatosensory	Left primary somatosensory cortex	Left precentral gyrus	42	7.39	−50	−20	38	−52.2	−19.4	38.4
Somatosensory	Left primary somatosensory cortex	Right inferior frontal gyrus	31	6.055	54	30	0	52.8	30.6	0.9
Somatosensory	Left secondary somatosensory cortex	Left cingulate gyrus	45	6.226	−16	24	44	−15.8	26.8	44.6
Somatosensory	Left secondary somatosensory cortex	Right supramarginal gyrus	42	5.734	48	−56	26	49.4	−57.1	23.4
Somatosensory	Left secondary somatosensory cortex	Right precentral gyrus	42	−8.503	50	−6	46	49	−3	45.3
Somatosensory	Left secondary somatosensory cortex	Right parahippocampal gyrus, right Brodmann area 36	37	6.936	28	−30	−22	31.5	−29.3	−21
	Left thalamus	Right thalamus, right ventral lateral nucleus	37	9.257	14	−16	16	15.5	−16.3	15.9
	Left thalamus	Left medial frontal gyrus (medial prefrontal cortex)	28	−5.806	−8	46	26	−3.1	49.2	30.2
DMN	Medial prefrontal cortex	Left medial frontal gyrus (medial prefrontal cortex)	67	−6.292	−10	22	48	−5.7	22.2	45.6
DMN	Medial prefrontal cortex	Left thalamus, left ventral posterior lateral nucleus	43	−6.81	−18	−22	6	−17.4	−22.2	6.5
DMN	Middle temporal gyrus	None								
DMN	Posterior cingulate/precuneus	Left cingulate gyrus (extends into right medial frontal gyrus, right middle frontal gyrus)	1127	10.251	−10	4	48	9.9	−1	53
DMN	Posterior cingulate/precuneus	Left middle frontal gyrus, left Brodmann area 6	230	10.608	−26	−2	50	−24.7	5	50
DMN	Posterior cingulate/precuneus	Right middle frontal gyrus	71	7.116	34	44	24	32	41.3	22.5
DMN	Posterior cingulate/precuneus	Right superior temporal gyrus	66	−5.881	54	−54	16	56.1	−53.2	11.1
DMN	Posterior cingulate/precuneus	Left cingulate gyrus, left Brodmann area 32	63	5.89	−6	22	38	−4	24.1	37.2
DMN	Posterior cingulate/precuneus	Right middle temporal gyrus, right Brodmann area 39	33	−6.148	56	−72	20	53	−68.9	19.4
Pain	Right nucleus accumbens	Right postcentral gyrus and right Brodmann area 3	42	6.606	54	−14	52	53.8	−15.1	52.8
Pain	Right nucleus accumbens	Left inferior frontal gyrus	29	6.635	−60	10	28	−59.9	9.2	25.7
Pain	Right anterior cingulate cortex	Left medial frontal gyrus (near subgenual cortex)	39	−9.31	−2	26	−14	0.3	26.1	−15
Pain	Right anterior cingulate cortex	Left middle temporal gyrus	37	5.479	−58	−66	10	−57.4	−65	7.6
Pain	Right anterior cingulate cortex	Right middle frontal gyrus	33	−8.333	52	34	24	50.3	34.5	26.5
Pain	Right amygdala	Left superior frontal gyrus, left Brodmann area 8	41	−7.856	−34	20	56	−34.5	21.3	54.3
Pain	Right dorsolateral prefrontal cortex	None								
Pain	Right orbital frontoinsula	Left inferior frontal gyrus, left Brodmann area 9	36	−6.061	−44	2	32	−45.3	2.8	33
Pain	Right orbital frontoinsula	Left middle temporal gyrus	30	7.414	−50	−46	−2	−49.8	−47.7	0.5
Pain	Right orbital frontoinsula	Left middle temporal gyrus	29	−5.703	−48	−8	−14	−46.3	−6	−16
Pain	Right posterior insula	Right claustrum	113	−11.135	32	−8	−6	33.5	−8.1	−0.9
Somatosensory	Right primary somatosensory cortex	Left precuneus	208	8.502	−10	−60	32	−2	−57.4	31.7
Somatosensory	Right primary somatosensory cortex	Right superior temporal gyrus	117	7.744	60	−58	18	56.9	−59.4	16.5
Somatosensory	Right primary somatosensory cortex	Left superior frontal gyrus	47	−7.997	−20	12	46	−20.7	10.4	47.5
Somatosensory	Right secondary somatosensory cortex	Left inferior parietal lobule	54	−14.204	−60	−38	30	−59.2	−38.3	28.6
Somatosensory	Right secondary somatosensory cortex	Right superior frontal gyrus	28	5.231	18	36	36	19.2	38.6	37.3
Somatosensory	Right secondary somatosensory cortex	Left postcentral gyrus, left Brodmann area 3	28	4.961	−22	−32	54	29.3	−32.4	54.9
	Right thalamus	Right cingulate gyrus, right Brodmann area 24	51	−6.372	6	0	38	5.7	1.1	37.3

The *t*-value and coordinates of the peak voxel in each cluster are given, along with the coordinates of the center of mass of each cluster. Coordinates are given in MNI space.
DMN, default mode network.

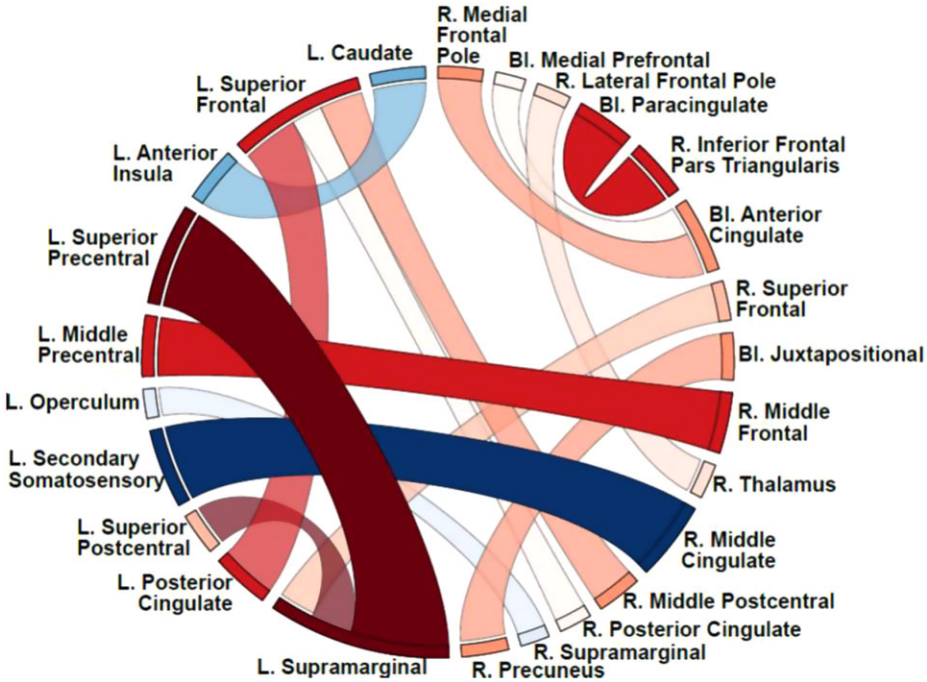

Figure 4. Differences in functional connectivity with spinal cord stimulation off or at optimal settings. Regions with functional connectivity that was stronger during optimal stimulation are shown in red, while functional connections that were weaker during optimal stimulation are shown in blue. The intensity of the color and thickness of the connection indicate the magnitude of the change in connectivity and are proportional to the *t*-value of the difference in functional connectivity.

neuropathic pain following lipomeningocele repair was noted following SCS in this study (22). Another study reported activation of the cingulate gyrus, thalamus, prefrontal cortex, supplementary motor area and post central gyrus when SCS was applied at the higher pain levels in three patients (24). Whereas no activation was noted in these areas following pain reduction with SCS in follow-up fMRI (24). Insular cortex has an extensive intrainsular connections and projections to different regions of the brain such as second somatosensory area and retroinsular area of the parietal lobe, orbital cortex, frontal operculum, lateral premotor cortex, ventral granular cortex, and medial area 6 in the frontal lobe, the superior temporal sulcus of the temporal lobe, amygdaloid nuclei, perirhinal cortex, entorhinal, and periamygdaloid cortex (36). Given these extensive connections, insular cortex is recognized as a somatosensory area, visceral sensory area, visceral motor area, motor association area emphasizing its importance in pain perception and processing (36,37). Secondary somatosensory cortex (S2) has been shown to have connections with subdivisions of anterior parietal cortex, motor and vasomotor fields of frontal cortex, parietal ventral area, and medial limbic cortex (38). Therefore, SCS may relieve neuropathic pain by modulating these pain processing nodal points.

DMN is the resting state network of the brain and consists of posterior cingulate cortex, medial frontal, precuneus, and lateral temporal cortex (39). DMN plays a key role in the cognitive aspects of pain perception (40) and is associated with functional connectivity hubs and brain networks (41). The resting DMN is abnormal in patients with chronic painful conditions implicating the impact of such chronic conditions on areas beyond pain perception (42–44). Tracey (20) described the pain endophenotypes in humans using neuroimaging techniques and reported the abnormalities in DMN/resting networks in addition to the effect of psychological factors, genetic influences, descending modulatory system, neurochemical tone, structural integrity resilience, and nociceptive input on pain perception in patients with chronic pain. Central processes such as memory and learning-related changes in the pain pathways/ networks with altered perception of body image have been implicated in the pathophysiology of chronic pain perception (21). In an experimental study, low back pain was induced with intramuscular injection of hypertonic saline in the back muscles and connectivity was analyzed using fMRI (43). Posterior cingulate cortex/precuneus showed greater functional connectivity when compared with the anterior cingulate cortex, lingual gyrus, and prefrontal regions as compared with baseline in this study (43). A significant decrease in functional connectivity was noted in cerebellum, the parahippocampal, and transverse temporal gyri (43). These findings reiterate the fact that the pain modulatory pathways and DMN are abnormal in patients with chronic pain. In our study, with optimal stimulator settings, increased connectivity was noted between somatosensory cortex and DMN, whereas increased connectivity was noted between somatosensory cortex and limbic networks when stimulator was turned OFF. These findings suggest that SCS tend to normalize the abnormal DMN and pain modulatory pathways in patients with chronic neuropathic pain.

Conventional fMRI using traditional methods by correlating the predictor and the canonical hemodynamic response function (HRF, the general linear model) may not detect all the brain regions involved in the pain processing (35). Newer innovative approaches such as inter-run synchronization (IRS) have been shown to detect areas responsible for pain processing which are otherwise not detectable using predictor-based analysis (35). These advances in imaging modalities will expand the understanding of pain perception.

Table 4. (a and b) Results of Whole Brain Analysis of Functional Connectivity Changes With Spinal Cord Stimulation Between Off and Optimal Settings.

a.

Data	R. Medial frontal pole	Bl. Medial prefrontal cortex	R. Lateral frontal pole	Bl. Paracingulate	R. Inferior frontal, pars triangularis	Bl. Anterior cingulate	R. Superior frontal	Bl. Juxtapositional	R. Middle frontal	R. Thalamus	R. Middle cingulate	R. Middle postcentral	R. Posterior cingulate
R. Medial frontal pole		–0.23	–1.19	–0.06	–0.09	**3.94**	0.36	–0.10	1.05	0.09	2.93	2.28	1.62
Bl. Medial prefrontal cortex	–0.23		–1.20	–1.36	–0.17	**3.44**	–0.07	–0.72	0.35	–0.32	0.72	1.12	2.21
R. Lateral frontal pole	–1.19	–1.20		1.12	–0.10	0.79	0.02	0.93	0.21	**3.60**	–1.36	–0.13	–0.05
Bl. Paracingulate	–0.06	–1.36	1.12		**4.34**	0.20	–0.49	0.36	–0.76	–0.09	–0.02	0.94	0.59
R. Inferior frontal, pars triangularis	–0.09	–0.17	–0.10	**4.34**		–1.19	2.63	0.27	–0.15	0.89	0.04	0.22	0.21
Bl. Anterior cingulate	**3.94**	**3.44**	0.79	0.20	–1.19		–0.46	–1.65	–1.50	1.22	0.26	–0.70	–0.08
R. Superior frontal	0.36	–0.07	0.02	–0.49	2.63	–0.46		–0.20	0.71	1.41	0.96	2.06	1.70
Bl. Juxtapositional	–0.10	–0.72	0.93	0.36	0.27	–1.65	–0.20		–0.10	0.91	–0.46	–1.77	1.55
R. Middle frontal	1.05	0.35	0.21	–0.76	–0.15	–1.50	0.71	–0.10		0.86	0.99	1.00	1.70
R. Thalamus	0.09	–0.32	**3.60**	–0.09	0.89	1.22	1.41	0.91	0.86		–0.83	0.23	0.30
R. Middle cingulate	2.93	0.72	–1.36	–0.02	0.04	0.26	0.96	–0.46	0.99	–0.83		–0.25	2.04
R. Middle postcentral	2.28	1.12	–0.13	0.94	0.22	–0.70	2.06	–1.77	1.00	0.23	–0.25		2.10
R. Posterior cingulate	1.62	2.21	–0.05	0.59	0.21	–0.08	1.70	1.55	1.70	0.30	2.04	2.10	
R. Supramarginal	0.01	–0.37	0.53	0.46	–0.05	–0.62	–0.07	–0.47	–0.89	0.88	–2.11	–0.33	–1.17
R. Precuneus	1.06	0.63	0.93	2.45	–0.09	1.31	3.18	**3.99**	1.07	–0.35	2.33	1.60	0.91
L. Supramarginal	1.10	1.27	–1.48	1.83	–0.01	0.59	**3.74**	2.29	3.29	0.24	1.78	2.37	1.78
L. Posterior cingulate	0.13	0.41	–0.62	1.34	0.53	1.62	2.11	2.01	2.43	0.84	2.50	1.83	0.80
L. Superior postcentral	1.01	1.52	–0.88	0.16	1.95	–0.12	0.42	0.48	0.73	1.31	1.25	2.28	1.22
L. Secondary somatosensory	–0.16	0.41	–0.64	–0.43	–0.42	–0.03	–0.45	–1.44	–0.57	0.22	**–4.89**	0.11	–1.07
L. Operculum	0.20	0.51	–0.37	0.14	–2.41	–0.57	–0.02	–1.48	–0.95	0.00	–1.19	–0.37	–0.04
L. Middle Precentral	0.14	–0.25	–1.56	2.12	0.09	–0.95	3.09	1.34	**4.44**	0.18	1.39	0.97	1.09
L. Superior precentral	1.01	1.04	0.18	0.74	0.49	–0.49	1.17	0.94	1.29	0.75	0.91	1.24	0.79
L. Anterior insula	0.39	–1.12	0.42	–1.24	–0.77	–0.24	–0.47	–1.10	–0.35	–0.48	–0.61	0.27	–0.81
L. Superior frontal	–0.33	–0.12	–0.62	–0.06	1.56	0.15	0.22	0.52	1.12	1.82	2.60	**3.91**	**3.54**
L. Caudate	0.08	–0.44	0.45	–0.88	–0.01	–0.06	–0.21	–0.22	–0.20	0.92	1.62	0.79	0.86

b.

Data	R. Supramarginal	R. Precuneus	L. Supramarginal	L. Posterior cingulate	L. Superior postcentral	L. Secondary somatosensory	L. Operculum	L. Middle precentral	L. Superior precentral	L. Anterior insula	L. Superior frontal	L. Caudate
R. Medial frontal pole	0.01	1.06	1.10	0.13	1.01	–0.16	0.20	0.14	1.01	0.39	–0.33	0.08
Bl. Medial prefrontal cortex	–0.37	0.63	1.27	0.41	1.52	0.41	0.51	–0.25	1.04	–1.12	–0.12	–0.44
R. Lateral frontal pole	0.53	0.93	–1.48	-0.62	–0.88	–0.64	–0.37	–1.56	0.18	0.42	–0.62	0.45
Bl. Paracingulate	0.46	2.45	1.83	1.34	0.16	–0.43	0.14	2.12	0.74	–1.24	–0.06	–0.88
R. Inferior frontal, pars triangularis	–0.05	–0.09	–0.01	0.53	1.95	–0.42	–2.41	0.09	0.49	–0.77	1.56	–0.01
Bl. Anterior cingulate	–0.62	1.31	0.59	1.62	–0.12	–0.03	–0.57	–0.95	–0.49	–0.24	0.15	–0.06
R. Superior frontal	–0.07	3.18	3.74	2.11	0.42	–0.45	–0.02	3.09	1.17	–0.47	0.22	–0.21
Bl. Juxtapositional	–0.47	3.99	2.29	2.01	0.48	–1.44	–1.48	1.34	0.94	–1.10	0.52	–0.22
R. Middle frontal	–0.89	1.07	3.29	2.43	0.73	–0.57	–0.95	4.44	1.29	–0.35	1.12	–0.20
R. Thalamus	0.88	–0.35	0.24	0.84	1.31	0.22	0.00	0.18	0.75	–0.48	1.82	0.92
R. Middle cingulate	–2.11	2.33	1.78	2.50	1.25	–4.89	–1.19	1.39	0.91	–0.61	2.60	1.62
R. Middle postcentral	–0.33	1.60	2.37	1.83	2.28	0.11	–0.37	0.97	1.24	0.27	3.91	0.79
R. Posterior cingulate	–1.17	0.91	1.78	0.80	1.22	–1.07	–0.04	1.09	0.79	–0.81	3.54	0.86
R. Supramarginal		–0.71	–0.18	–2.24	–0.09	–1.78	–3.42	–1.52	–0.86	–3.34	0.36	–1.56
R. Precuneus	–0.71		–0.22	1.32	3.01	–0.37	0.89	2.79	2.30	–0.73	2.78	1.32
L. Supramarginal	–0.18	–0.22		2.35	3.84	–0.64	–0.34	2.05	5.42	–0.61	3.18	2.07
L. Posterior cingulate	–2.24	1.32	2.35		1.35	–2.08	–1.71	0.42	1.88	–1.57	4.33	1.22
L. Superior postcentral	–0.09	3.01	3.84	1.35		–0.07	0.14	0.81	0.26	0.27	1.01	0.33
L. Secondary somatosensory	–1.78	–0.37	–0.64	–2.08	–0.07		–1.24	–1.46	–1.56	–0.09	0.04	–0.52
L. Operculum	–3.42	0.89	–0.34	–1.71	0.14	–1.24		–1.33	–1.23	–0.01	–0.71	–1.04
L. Middle precentral	–1.52	2.79	2.05	0.42	0.81	–1.46	–1.33		2.17	–1.11	2.40	0.06
L. Superior precentral	–0.86	2.30	5.42	1.88	0.26	–1.56	–1.23	2.17		–1.06	1.62	0.78
L. Anterior insula	–3.34	–0.73	–0.61	–1.57	0.27	–0.09	–0.01	–1.11	–1.06		0.06	–4.23
L. Superior frontal	0.36	2.78	3.18	4.33	1.01	0.04	–0.71	2.40	1.62	0.06		0.50
L. Caudate	–1.56	1.32	2.07	1.22	0.33	–0.52	–1.04	0.06	0.78	–4.23	0.50	0.00

This symmetric matrix shows the *t*-values for the differences in correlation between off and optimal settings for each pair of regions. Only regions that had at least one significantly different connection are shown. Values in bold indicate *t*-values that met a false discovery rate threshold of 5%.

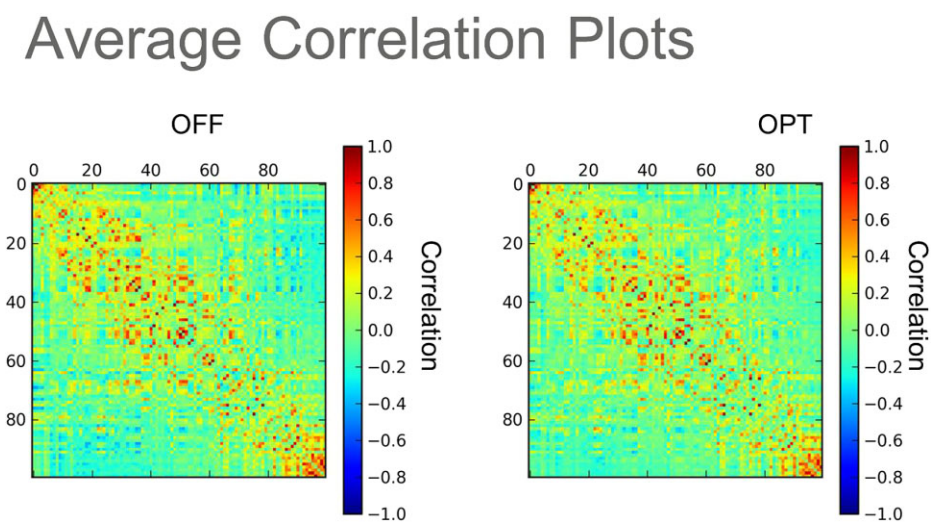

Figure 5. Figure shows an average pairwise correlation between 100 regions of interest during the stimulator OFF and optimal state.

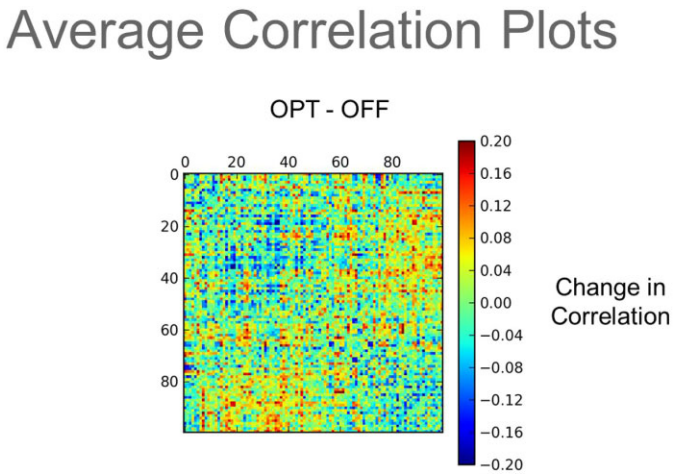

Figure 6. Figure shows average change in correlation across all subjects during the stimulator OFF and optimal state.

fMRI Safety

In this study, we have used a transmit/receive (T/R) head-coil and limited the lead tip locations to the thoracic region. This combination greatly reduced the risk by separating the area of the body, which was exposed to radio-frequency (RF) energy from that which contains the lead. The second limiting factor reducing the potential for lead heating was the low B_1rms implemented in the proposed scans. Lead heating is proportional to B_1rms^2 and therefore the risk of lead heating can be directly controlled by limiting its value.

To assess safety and maintain a low level of risk to the patient, the gradient environment was accurately defined for the specific MR equipment, scan sequences, and implant locations listed in the study. This was accomplished by a combination of direct dB/dt measurements and electromagnetic simulations. The electromagnetic field can then be accurately determined at the device as well as along the lead path. The risk of device failure from exposure to MRI electromagnetic fields, above and beyond the levels used in this study, was extensively examined with the device in the "off" positions through Discrete Cosine Transform testing. The standard radiated and injected gradient electromagnetic compatibility (EMC) testing was performed with the device in the "on" state at levels dictated by the specific gradient environment to assess risk. Due to the low levels of RF exposure, additional RF EMC testing was not required.

Limitations

There are certain limitations of our study. First, the heterogeneous population of patients was enrolled in this study. Second, subjective quantification of pain using VAS was used in this study. Third, collinear stimulation setting was used in all the patients. Fourth, it was difficult to blind the patients in our study. Another limitation was that the patients with early response (within 10 min) to the SCS were included in this study, excluding those with delayed or carry-over effect, which may not represent the true sample of all the patients with SCS. This was potentially unavoidable due to required study methods and due to reported variations in the carry-over effect of SCS (45). Nonetheless, our study provides insights into the mechanism of SCS and cortical connectivity.

CONCLUSION

Pain relief from SCS is secondary to reduced connectivity between the somatosensory and limbic networks. This suggests that effective SCS reduces negative emotional processing associated with pain, allowing somatosensory areas to become more integrated into default mode activity and normalization of brain networks. In addition, fMRI can be safely performed with SCS. However, randomized controlled studies with larger sample size are required to validate these findings.

Acknowledgements

Medtronic provided funding for the study and statistical support in analyzing the data, with input from Drs. Dylan M. Nielson, Xiangyu Yang, Louis Vera-Portocarrero, Gregory F. Molnar, Amir Abduljalil, and Per B. Sederberg; and also provided funding for editorial support.

Authorship Statements

Drs. Milind Deogaonkar, Mayur Sharma, Chima Oluigbo, Dylan Nielson, Xiangyu Yang; Louis Vera-Portocarrero, Gregory F. Molnar, Amir Abduljalil, Per Sederberg, Michael Knop, and Ali Rezai designed and conducted the study, including patient recruitment, data collection, and data analysis. Drs. Mayur Sharma and Milind Deogaonkar prepared the manuscript draft with important intellectual input from Drs. Xiangyu Yang, Amir Abduljalil, Dylan Nielson, and Ali Rezai. All authors approved the final manuscript. Drs. Milind Deogaonkar, Xiangyu Yang, Dylan Nielson, Amir Abduljalil, Per Sederberg, Michael Knop, and Ali Rezai had complete access to the study data. We would like to thank Dr. Ali Rezai for his editorial support during preparation of this manuscript.

How to Cite this Article:

Deogaonkar M., Sharma M., Oluigbo C., Nielson D.M., Yang X., Vera-Portocarrero L., Molnar G.F., Abduljalil A., Sederberg P.B., Knopp M., Rezai A. 2016. Deep Brain Spinal Cord Stimulation (SCS) and Functional Magnetic Resonance Imaging (fMRI): Modulation of Cortical Connectivity With Therapeutic SCS.
Neuromodulation 2016; 19: 142–153

REFERENCES

1. Dworkin RH. An overview of neuropathic pain: syndromes, symptoms, signs, and several mechanisms. *Clin J Pain* 2002;18:343–349.
2. Merskey H, Bogduk N. *Classification of chronic pain. Descriptions of chronic pain syndromes and definitions of pain terms*, 2nd ed. Seattle: IASP Press, 1994.
3. Van Boxem K, Cheng J, Patijn J et al. 11. Lumbosacral radicular pain. *Pain Pract* 2010;10:339–358.
4. Breivik H, Collett B, Ventafridda V, Cohen R, Gallacher D. Survey of chronic pain in Europe: prevalence, impact on daily life, and treatment. *Eur J Pain* 2006;10:287–333.
5. Reinders MF, Geertzen JH, Dijkstra PU. Complex regional pain syndrome type I: use of the International Association for the Study of Pain diagnostic criteria defined in 1994. *Clin J Pain* 2002;18:207–215.
6. Kumar K, Hunter G, Demeria D. Spinal cord stimulation in treatment of chronic benign pain: challenges in treatment planning and present status, a 22-year experience. *Neurosurgery* 2006;58:481–496, discussion 481–496.
7. Kumar K, Malik S, Demeria D. Treatment of chronic pain with spinal cord stimulation versus alternative therapies: cost-effectiveness analysis. *Neurosurgery* 2002;51:106–115, discussion 115–106.
8. Kumar K, North R, Taylor R et al. Spinal cord stimulation vs. conventional medical management: a prospective, randomized, controlled, multicenter study of patients with failed back surgery syndrome (PROCESS Study). *Neuromodulation* 2005;8:213–218.
9. Kumar K, Taylor RS, Jacques L et al. Spinal cord stimulation versus conventional medical management for neuropathic pain: a multicentre randomised controlled trial in patients with failed back surgery syndrome. *Pain* 2007;132:179–188.
10. Kumar K, Taylor RS, Jacques L et al. The effects of spinal cord stimulation in neuropathic pain are sustained: a 24-month follow-up of the prospective randomized controlled multicenter trial of the effectiveness of spinal cord stimulation. *Neurosurgery* 2008;63:762–770, discussion 770.
11. Linderoth B, Foreman RD. Physiology of spinal cord stimulation: review and update. *Neuromodulation* 1999;2:150–164.
12. Meyerson BA, Linderoth B. Mode of action of spinal cord stimulation in neuropathic pain. *J Pain Symptom Manage* 2006;31 (4 Suppl.):S6–S12.
13. Meyerson BA, Linderoth B. Mechanisms of spinal cord stimulation in neuropathic pain. *Neurol Res* 2000;22:285–292.
14. Oakley JC, Prager JP. Spinal cord stimulation: mechanisms of action. *Spine (Phila Pa 1976)* 2002;27:2574–2583.
15. Saade NE, Atweh SF, Privat A, Jabbur SJ. Inhibitory effects from various types of dorsal column and raphe magnus stimulations on nociceptive withdrawal flexion reflexes. *Brain Res* 1999;846:72–86.
16. El-Khoury C, Hawwa N, Baliki M, Atweh SF, Jabbur SJ, Saade NE. Attenuation of neuropathic pain by segmental and supraspinal activation of the dorsal column system in awake rats. *Neuroscience* 2002;112:541–553.
17. Melzack R. From the gate to the neuromatrix. *Pain* 1999; (Suppl. 6):S121–S126.
18. Friebel U, Eickhoff SB, Lotze M. Coordinate-based meta-analysis of experimentally induced and chronic persistent neuropathic pain. *Neuroimage* 2011;58:1070–1080.
19. Peyron R, Faillenot I. [Functional brain mapping of pain perception]. *Med Sci (Paris)* 2011;27:82–87.
20. Tracey I. Can neuroimaging studies identify pain endophenotypes in humans? *Nat Rev Neurol* 2011;7:173–181.
21. Flor H. New developments in the understanding and management of persistent pain. *Curr Opin Psychiatry* 2012;25:109–113.
22. Kiriakopoulos ET, Tasker RR, Nicosia S, Wood ML, Mikulis DJ. Functional magnetic resonance imaging: a potential tool for the evaluation of spinal cord stimulation: technical case report. *Neurosurgery* 1997;41:501–504.
23. Stancak A, Kozak J, Vrba I et al. Functional magnetic resonance imaging of cerebral activation during spinal cord stimulation in failed back surgery syndrome patients. *Eur J Pain* 2008;12:137–148.
24. Rasche D, Siebert S, Stippich C et al. Spinal cord stimulation in Failed-Back-Surgery-Syndrome. Preliminary study for the evaluation of therapy by functional magnetic resonance imaging (fMRI). *Schmerz* 2005;19:497–500, 502–495.
25. Jensen TS, Baron R, Haanpaa M et al. A new definition of neuropathic pain. *Pain* 2011;152:2204–2205.
26. Ohnhaus EE, Adler R. Methodological problems in the measurement of pain: a comparison between the verbal rating scale and the visual analogue scale. *Pain* 1975;1:379–384.
27. Aicher B, Peil H, Peil B, Diener HC. Pain measurement: visual analogue scale (VAS) and verbal rating scale (VRS) in clinical trials with OTC analgesics in headache. *Cephalalgia* 2012;32:185–197.
28. Boonstra AM, Schiphorst Preuper HR, Reneman MF, Posthumus JB, Stewart RE. Reliability and validity of the visual analogue scale for disability in patients with chronic musculoskeletal pain. *Int J Rehabil Res* 2008;31:165–169.
29. Biswal BB, Mennes M, Zuo XN et al. Toward discovery science of human brain function. *Proc Natl Acad Sci U S A* 2010;107:4734–4739.
30. Smith SM, Jenkinson M, Woolrich MW et al. Advances in functional and structural MR image analysis and implementation as FSL. *Neuroimage* 2004;23 (Suppl. 1):S208–S219.
31. Cox RW. AFNI: software for analysis and visualization of functional magnetic resonance neuroimages. *Comput Biomed Res* 1996;29:162–173.
32. Duerden EG, Albanese MC. Localization of pain-related brain activation: a meta-analysis of neuroimaging data. *Hum Brain Mapp* 2013;34:109–149.
33. Strimmer K. fdrtool: a versatile R package for estimating local and tail area-based false discovery rates. *Bioinformatics* 2008;24:1461–1462.
34. Craddock RC, James GA, Holtzheimer PE 3rd, Hu XP, Mayberg HS. A whole brain fMRI atlas generated via spatially constrained spectral clustering. *Hum Brain Mapp* 2012;33:1914–1928.
35. Cauda F, Costa T, Diano M, Duca S, Torta DM. Beyond the "Pain Matrix," inter-run synchronization during mechanical nociceptive stimulation. *Front Hum Neurosci* 2014;8:265.
36. Augustine JR. Circuitry and functional aspects of the insular lobe in primates including humans. *Brain Res Brain Res Rev* 1996;22:229–244.
37. Frot M, Mauguiere F. Dual representation of pain in the operculo-insular cortex in humans. *Brain* 2003;126 (Pt 2):438–450.
38. Krubitzer LA, Kaas JH. The organization and connections of somatosensory cortex in marmosets. *J Neurosci* 1990;10:952–974.
39. Raichle ME, MacLeod AM, Snyder AZ, Powers WJ, Gusnard DA, Shulman GL. A default mode of brain function. *Proc Natl Acad Sci U S A* 2001;98:676–682.
40. Buckner RL, Andrews-Hanna JR, Schacter DL. The brain's default network: anatomy, function, and relevance to disease. *Ann N Y Acad Sci* 2008;1124:1–38.
41. Tomasi D, Volkow ND. Association between functional connectivity hubs and brain networks. *Cereb Cortex* 2011;21:2003–2013.
42. Tagliazucchi E, Balenzuela P, Fraiman D, Chialvo DR. Brain resting state is disrupted in chronic back pain patients. *Neurosci Lett* 2010;485:26–31.
43. Zhang S, Wu W, Huang G et al. Resting-state connectivity in the default mode network and insula during experimental low back pain. *Neural Regen Res* 2014;9:135–142.
44. Otti A, Guendel H, Henningsen P, Zimmer C, Wohlschlaeger AM, Noll-Hussong M. Functional network connectivity of pain-related resting state networks in somatoform pain disorder: an exploratory fMRI study. *J Psychiatry Neurosci* 2013;38:57–65.
45. Gong W, Johanek LM, Sluka KA. Spinal cord stimulation reduces mechanical hyperalgesia and restores physical activity levels in animals with noninflammatory muscle pain in a frequency-dependent manner. *Anesth Analg* 2014;119:186–195.

COMMENTS

This is an interesting study using resting state functional MRI (rs-fMRI) to demonstrate the effects of spinal cord stimulation (SCS) on cortical activation. Patients were used as their own controls and when their SCS was activated, decreased somatosensory/limbic activation was identified and increased somatosensory/default mode activation was identified. This correlated with patients' self-report of pain improvement. The study is well described with sound methods.

rs-fMRI has evolved to an accurate and reproducible neuroimaging technique. As demonstrated in the present study, it may potentially be used as a surrogate marker for pain level in chronic pain states. In the present study rs-fMRI is used to demonstrate treatment effect; however, it also may potentially be used for diagnosis. Further, rs-fMRI may identify patients with patterns of somatosensory/limbic interaction best suited for a particular intervention. A sound knowledge base of expected rs-fMRI activation patterns before and after treatment in various chronic pain conditions is necessary to fully utilize this neuroimaging tool. The present manuscript is a welcome step toward that goal.

Andrew J. Fabiano, MD
Buffalo, NY, USA

***

Working mechanisms of SCS despite advances in research methods are still largely not understood. FMRI techniques provide an opportunity for researchers to map and code cortical activity and changes in cortical activity in response to treatment techniques. The reported use of FMRI with respect to SCS is limited to a handful of studies. This study uses FMRI to explore the potential impact of SCS with respect to cortical pain processing for management of neuropathic leg pain and CRPS.

Selina Johnson, MSc, BSc (Hons)
Liverpool, United Kingdom

***

This is a paper on the changes in connectivity of different parts of the brain in response to spinal cord stimulation in patients with chronic pain in the legs. The authors looked at brain connectivity using functional MR imaging and found that pain relief that was associated with the stimulator being "on" was associated with decreased connectivity between parts of the brain that were the first to receive electrical signals activated by pain (so-called somatosensory regions) and limbic areas that receive stimuli secondarily and "assign" emotional reactions to the pain. In contrast the active stimulator being "on" was associated with increased connectivity between somatosensory areas of the brain and the so-called "default mode network" which is usually active in a state of "wakeful rest" when the patient is in a state of wakeful rest.

These results suggest that the stimulator being "on" changes the brain's network properties so there is a primary perception of pain but the patient does not perceive it as noxious and emotionally taxing or unpleasant.

Michael Johnson, MD
Baltimore, MD, USA

Comments not included in the Early View version of this paper.

